Low Temperature Physics/Fizika Nizkikh Temperatur, 2015, v. 41, No. 9, pp. 942–948

Discrete breathers in an one-dimensional array of magnetic dots

Roman L. Pylypchuk[1] and Yaroslav Zolotaryuk[2]

[1]*Physics Department, Ludwig-Maximilians-Universität, Theresienstrasse 37, 80333 München, Germany*

[2]*Bogolyubov Institute for Theoretical Physics, National Academy of Sciences of Ukraine, Kyiv, 03680, Ukraine*
E-mail: yzolo@bitp.kiev.ua

Received April 16, 2015, published online July 24, 2015

The dynamics of the one-dimensional array of magnetic particles (dots) with the easy-plane anisotropy is investigated. The particles interact with each other via the magnetic dipole interaction and the whole system is governed by the set of Landau–Lifshitz equations. The spatially localized and time-periodic solutions known as discrete breathers (or intrinsic localized modes) are identified. These solutions have no analogue in the continuum limit and consist of the core where the magnetization vectors precess around the hard axis and the tails where the magnetization vectors oscillate around the equilibrium position.

PACS: 63.20.Pw Localized modes;
63.20.Ry Anharmonic lattice modes;
75.10.Hk Classical spin models.

Keywords: magnetic dots, antiferromagnets, Landau–Lifshitz equations.

1. Introduction

The artificially manufactured periodic arrays of magnetic particles have received much attention in the literature during the last two decades [1–8]. Apart from their technological importance as candidates for the high-density magnetic storage media [1,2,5], these arrays appear to be a good testing ground for studying various nonlinear magnetic wave phenomena [9–11].

Many of these phenomena, such as magnetic solitons, domain walls, vortices are well studied and documented in scientific literature [12,13]. Owing to the fact that they are well described by the continuum version of the Landau-Lifshitz (LL) equation, these solutions can be treated analytically. In some cases, if the underlying system is integrable, the inverse scattering method has been applied [14]. The anharmonic localization in lattices occupies a special place among other nonlinear wave phenomena. The discrete breathers (DBs) (also know as intrinsic localized modes) [15–21] are time-periodic and spatially localized excitations. Unlike their continuum counterparts that normally exist only in the integrable systems [22], discrete breathers can exist in discrete media that are not necessarily described by the integrable equations. Discrete breathers owe their existence to the fact that the spectrum of the linear waves is bounded and as a result all the resonances with the linear excitations can be avoided if the breather frequency and/or the system parameters are chosen appropriately [23,24]. In magnetic systems DBs have been studied rather extensively [20,25–33]. In particular, experimental observation of breathers in antiferromagnets has been reported [34,35].

The bulk of these studies was performed for the Heisenberg magnets, where the interaction between the neighbouring spins occurs via the exchange interaction. For the Heisenberg models the exchange interaction usually dominates over the single-ion anisotropies, so the breather solutions in the underlying models can be treated as the weakly discrete modes. Also, interesting solutions that have no analogue in the continuum limit has been discussed [29,30,36,37]. The weakness of the interspin interaction comparing to the anisotropy (or they should be at least of the same order) is necessary for these excitations. In the magnetic dots arrays the interaction between the dots is of the dipole-dipole kind, which decays as r^{-3} (with r being the distance between the interacting magnets). Thus, if the array is manufactured with the spacing large enough to guarantee the fulfilment of the necessary non-resonance conditions, it is highly probable that DBs will exist in such a system. To investigate the DB existence in the magnetic dot array is the main aim of this article.

The paper is organized as follows. In the first section the model of interacting magnetic dipoles is presented. The next section is devoted to the numerical studies of discrete breathers. Discussion and conclusions are given in the last section.

2. The model

2.1. The Hamiltonian and equations of motion

We consider the one-dimensional array of N immobile equidistant magnetic particles that interact as magnetic dipoles.

The Hamiltonian of this model consists of the dipole-dipole interaction energy between all dots and the magnetic anisotropy term for each dot [38]:

$$H = \frac{1}{2a^3}\sum_{m\neq n}^{N}\frac{(\mathbf{M}_n, \mathbf{M}_m) - 3(\mathbf{v}_{mn}, \mathbf{M}_n)(\mathbf{v}_{mn}, \mathbf{M}_m)}{|m-n|^3} - D\sum_{n=1}^{N}\mathbf{M}_n^{z2}. \tag{1}$$

Here D is the anisotropy constant, a is the distance between the adjacent dots, $\mathbf{v}_{mn} \equiv \mathbf{e}_x$, and $\mathbf{M}_n = (M_n^x, M_n^y, M_n^z)^T$ ($|\mathbf{M}_n|^2 = M^2$) is the magnetic dipole momentum of the nth particle. In this article the easy-plane anisotropy is considered with the plane of the array (xy) being the easy plane, thus, $D < 0$.

It is convenient to introduce the new dimensionless variables in which the total magnetic dipole momentum is normalized to unity:

$$\boldsymbol{\mu}_n = \mathbf{M}_n/M, \quad \bar{H} = H/|D|M^2, \quad t \to 2\gamma|D|Mt. \tag{2}$$

In the new dimensional variables the dynamics of the magnetic moment of the nth dot is described by the discrete version of the LL equation [38]:

$$\dot{\boldsymbol{\mu}}_n = [\nabla_{\boldsymbol{\mu}_n}\bar{H} \times \boldsymbol{\mu}_n],$$

$$\nabla_{\boldsymbol{\mu}_n} = \mathbf{e}_x\frac{\partial}{\partial\mu_n^{(x)}} + \mathbf{e}_y\frac{\partial}{\partial\mu_n^{(y)}} + \mathbf{e}_z\frac{\partial}{\partial\mu_n^{(z)}}, \tag{3}$$

where the dot denotes differentiation with respect to time. Now the system of coupled dipoles has only one parameter: $\chi = 1/(2|D|a^3)$. This parameter appears as a prefactor in the dipole-dipole term of the dimensionless energy $\bar{H}$. It can be treated either as a measure of the discreteness of the system or as the ratio of the dipole-dipole and exchange energies.

2.2. Dispersion law

Before embarking on studies of the nonlinear vibrations of the array it is useful to recall the dispersion law of the linear waves (magnons). The magnon spectrum can be found when Eq. (3) is linearized around the obvious ground state, where the dipoles are lying in the easy plane and are oriented tail-to-tail: $\mu_n^{(x)} = 1$, $\mu_n^{(y)} = \mu_n^{(z)} = 0$. Consider first the infinite array. Then the dispersion law is well-known and reads [7,11]

$$\omega_L^2(q) = 2\chi\sum_{n=1}^{\infty}\frac{\cos(nq)+2}{n^3}\left[2\chi\sum_{n=1}^{\infty}\frac{\cos(nq)+2}{n^3}+1\right]. \tag{4}$$

Typical curves for the dispersion law for the different values of the coupling constant χ are given in Fig. 1(a). If the array is finite the magnon band becomes discrete. It consists of the set of modes $\omega_L^{(n)}$, $n = 1, 2, \ldots, N$. The dependence of these modes as a function of the coupling constant is given in Fig. 1(b). Strictly speaking, the discrete translational invariance is lost for the finite linear array and we can speak about it only in the approximate sense if χ is small. As a result, there is a mode that is placed below the band (see Fig. 1(b)). If the periodic boundary conditions are applied the translational invariance of the array holds exactly.

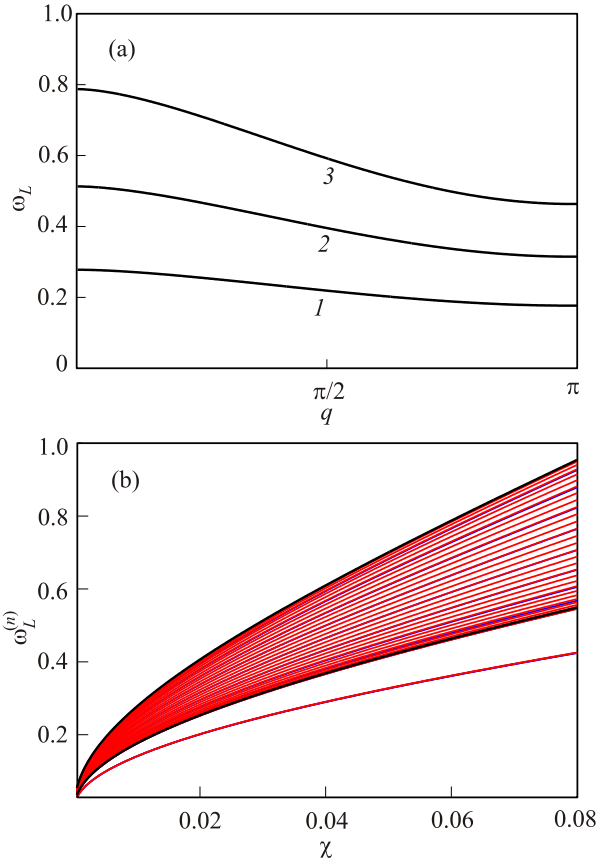

Fig. 1. (Color online) Dispersion law (4) for χ = 0.01 (curve *1*), χ = 0.03 (curve *2*) and χ = 0.06 (curve *3*) (a). Frequencies of the magnon modes as a function of χ for the finite chain with N = 11 (blue) and N = 31 (red). Thick black lines demonstrates $\omega_L(0)$ and $\omega_L(\pi)$ from Eq. (4) (b).

3. Discrete breathers and their properties

In this section we report the results of the studies of discrete breathers with the help of numerical simulations.

3.1. Spontaneous localization

Discrete breathers are spatially localized excitations that are periodic in time, i.e. $\{\boldsymbol{\mu}_n(t)\}_{n=1}^N = \{\boldsymbol{\mu}_n(t+T)\}_{n=1}^N$, $T = 2\pi/\omega$, where ω is the breather frequency. The concept of the anti-continuum limit [17,18] is important for constructing the DB solutions. In the current model it can be implemented by setting $\chi = 0$. Thus, the dipole-dipole interaction between the dots is absent and each of them can be excited independently. If a particular dot with the number $n = n_0$ is excited, the magnetization vector will perform precession around the hard axis with the frequency $\omega = \mu_{n_0}^{(z)}$. Projection on the xy plane demonstrates the following dynamics: $\mu_{n_0}^{(x)} + i\mu_{n_0}^{(y)} = = \sqrt{1-\omega^2}\, e^{i(\omega t+\varphi)}$. Similarly, several dots located in the arbitrary places of the array, can be excited.

In this article we will restrict ourselves to the configurations that consist of the precessing core of N_r dipoles. Such an initial state can be represented as follows:

$$\mathrm{m}^{(0)} = \left\{ \begin{bmatrix}1\\0\\0\end{bmatrix}, \begin{bmatrix}1\\0\\0\end{bmatrix}, \ldots, \begin{bmatrix}1\\0\\0\end{bmatrix}, \underbrace{\begin{bmatrix}\sqrt{1-\omega^2}\cos\varphi\\ \sqrt{1-\omega^2}\sin\varphi\\ \omega\end{bmatrix}, \ldots, \begin{bmatrix}\sqrt{1-\omega^2}\cos\varphi\\ \sqrt{1-\omega^2}\sin\varphi\\ \omega\end{bmatrix}}_{n=n_0,\ldots,n_0+N_r} \begin{bmatrix}1\\0\\0\end{bmatrix}, \ldots \begin{bmatrix}1\\0\\0\end{bmatrix}, \begin{bmatrix}1\\0\\0\end{bmatrix} \right\}. \tag{5}$$

First of all we report on the simple numerical experiment that demonstrates the phenomenon of dynamical localization of the magnetic dot magnetization. We take the anti-continuum configuration $\mathbf{m}^{(0)}$ from Eq. (5) as the initial condition and integrate the LL equations numerically. The fourth order Runge–Kutta method was used. The precision of the method was tested by monitoring the conservation of the total energy and the dipole moment. We have observed different results that depend on the value of χ. If this constant is sufficiently small, the localized state

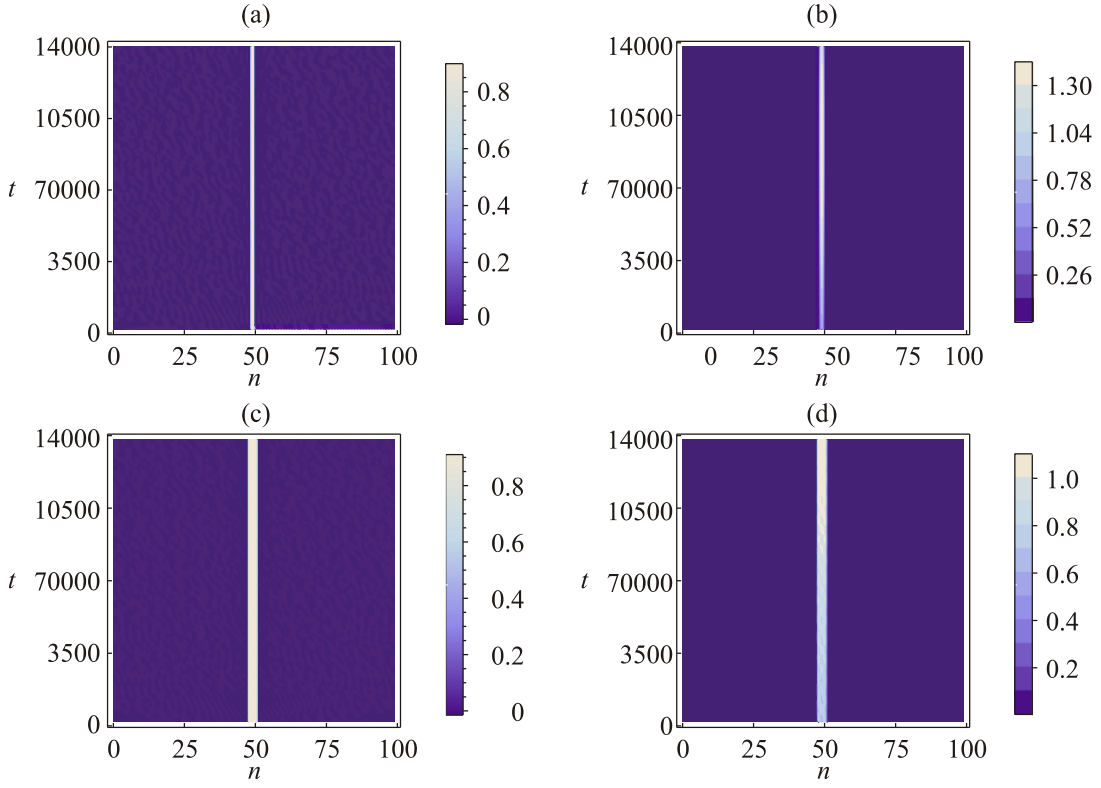

Fig. 2. (Color online) Contour plots of the temporal evolution of the $\mu_n^{(z)}$ (a), (c) and $1-\mu_n^{(x)}$ (b), (d) components of the magnetization in the array of $N = 100$ magnetic dots with the initially excited one [(a), (b), $\chi = 0.039$] and three [(c), (d), $\chi = 0.0045$] dipoles.

persists for rather long times. Otherwise, for larger values of χ the initially excited dipoles fall into the easy plane and localization disappears. In Fig. 2 the contour plots of the dynamical evolution of the array magnetization are demonstrated for $N_r = 1$ [panels (a), (b)] and $N_r = 3$ [panels (c), (d)] initially excited dots. Here the dipoles were initially excited with $\mu_n^{(z)} = 0.9$. As one can see, energy stays with the initially excited central dots remain in the excited state for rather long time, with the respective magnetization vectors precessing around the hard axis. The lifetime of the localized excitation exceeds the period of one rotation $T \simeq 2\pi/0.9 \simeq 7$ by several orders of magnitude. Thus, the phenomenon of dynamical localization is established. At this point we wish to know whether a localized mode is an exact periodic solution that can be attributed to the excitations known as discrete breathers [19]. Below we investigate these excitations in more detail.

3.2. Breather periodic orbits

In this subsection we show that time-periodic localized modes are indeed exact solutions of the LL equation. Numerically this task can be performed in the following way. Define the evolution operator

$$\hat{I}_T : \mathrm{m}(t_0) \to \mathrm{m}(t_0 + T), \ \mathrm{m} = \mathrm{col}(\boldsymbol{\mu}_1, \boldsymbol{\mu}_2, \ldots, \boldsymbol{\mu}_N), \quad (6)$$

which stands for the integration of the LL equations (3) along the time interval $[t_0, t_0 + T]$. The fixed points of the $3N$-dimensional map

$$\boldsymbol{\mu}_\mathbf{n}(t_0 + T) - \boldsymbol{\mu}_\mathbf{n}(t_0) + |\boldsymbol{\mu}_n(t_0 + T)|^2 - 1 = 0, n = 1, 2, \ldots, N, \quad (7)$$

will be the periodic solution with the period T. This map is complemented by the term $|\boldsymbol{\mu}_n(t_0 + T)|^2 - 1$, which is necessary to ensure that the normalization condition holds after each iteration step. We start from the anti-continuum

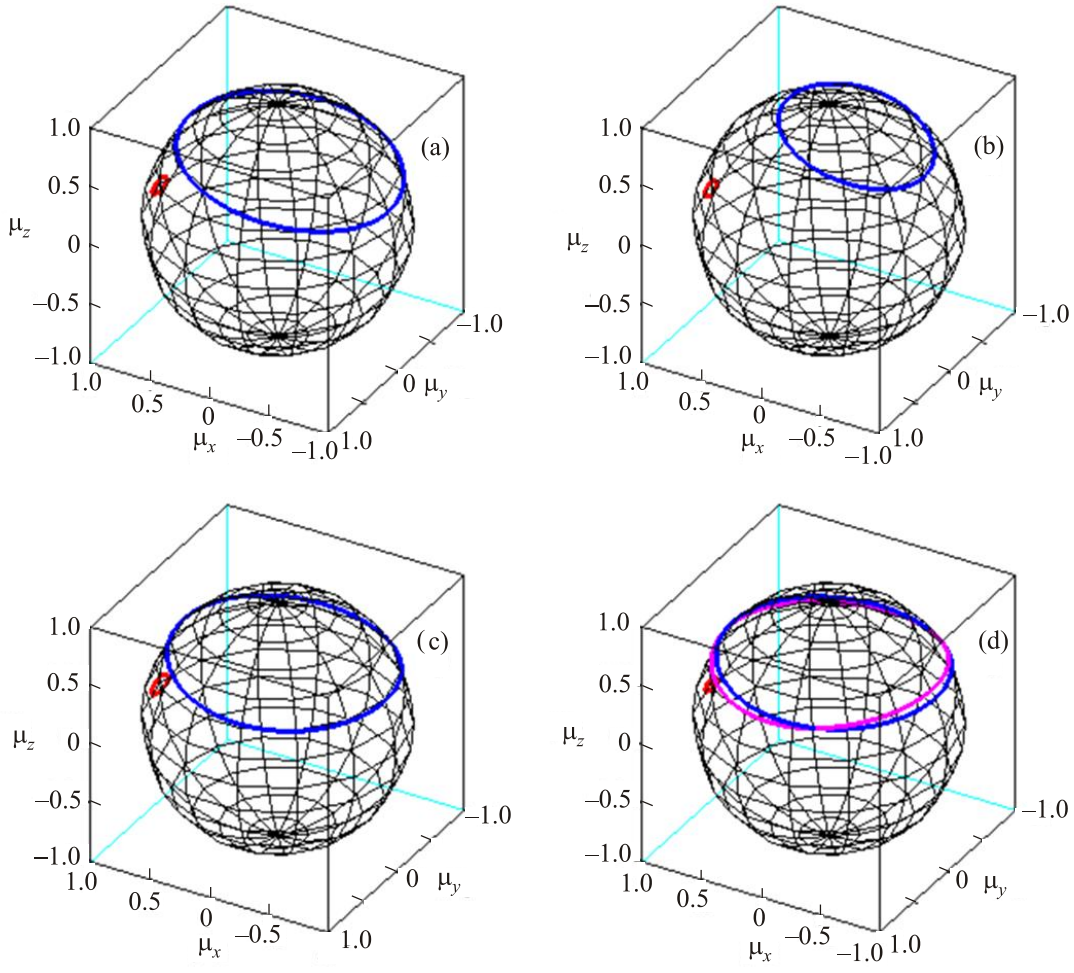

Fig. 3. (Color online) Dynamics of the central out-of-plane and neighbouring magnetization vectors of the DB orbit on the unit sphere for: (a) blue curve (central dot, n = 16), red curve (n = 15), other parameters χ = 0.022, ω = 0.5, N = 31; (b) same as (a) but for χ = 0.048, ω = 0.75; (c) same as (a) but for N = 20 dots with N_r = 2, blue curves correspond to the dots n = 10 and n = 11, red curve : n = 9; (d) N = 21 dots with N_r = 3, ω = 0.5, χ = 0.016, pink curve corresponds to n = 11, blue curves n = 10 and n = 12, red curve: n = 9.

limit (5), "turn on" the dipole-dipole interaction by setting $\chi > 0$ and show that the spatially localized excitation persist. Then χ can be increased gradually and the breather periodic orbit can be followed until it ceases to exist. In case of successful choice of the initial configuration $\mathrm{m}(t_0)$ convergence with the desired precision takes place after several iteration steps. The numerical scheme based on the Newton method [39] has been designed [40] for finding DB periodic oribits. It has been shown to work successfully in the number of models [41], including magnetic lattices [29,30]. Below we report the main results.

Starting from the anti-continuum approximation (5) and using the method, described above, we have managed to detect the breather periodic orbits for the different values of χ and ω, number of dots in the array N, and number of the precessing dipoles, N_r. The phase φ in the initial condition $\mathrm{m}^{(0)}$ does not seem to play any role as we have achieved conversion to the same solutions for the different values of φ. The dynamics of the magnetization vector $\boldsymbol{\mu}_n$ of these periodic orbits is shown in Fig. 3. The structure of DB's in all these figures is the same: it consists of the core of few dipoles that precess around the hard axis (although due to the interaction the precession trajectory is tilted towards the x axis) and the weakly oscillating tails. If the coupling constant χ is increased, the precessing trajectory is tilted stronger toward the x axis as the in-plane dipoles interact stronger with the precessing dipole (compare Figs. 3(a) and 3(b)). Note, that the oscillations beyond the precessing core appear to be rather weak (shown by the red trajectories).

Next we estimate the existence area of DBs on the parameter plane (χ,ω). We remind that in order to exist, the breather frequency together with its multiples should not resonate with the linear waves of the system. In the anti-continuum limit $(\chi = 0)$ the allowed range of the breather frequencies is $0 < \omega < 1$. Since the precession frequency coincides with the z component of the magnetization vector, ω cannot exceed 1. If the coupling is on, the allowed breather frequencies lie in the range $\max_{q\in[0,\pi]}\omega_L(q) < \omega < 1$. Thus, the existence area of DBs in the (χ,ω) parameter plane coincides approximately with the upper left triangle in Fig. 2(b) with the edges, given by $\omega = 1$, $\chi = 0$ and $\omega = \omega_L^{(N)}$. We have managed to track numerically the DB periodic orbit starting from $\chi = 0$ up to the critical values when the Newton method ceases to exist. We have found the orbits to persist into the magnon spectrum. In that case the breather tails do not decay asymptotically as $n \to 0, N$. Instead, we observe a bound breather-magnon state. However, these solutions appear to be unstable.

The asymptotic behaviour of the breather tails is given in Fig. 4. The decay law is close to the power law if we are not far from the anti-continuum limit. Indeed, we observe almost power law decay for $\chi = 0.018$ with $1-\mu_n^{(x)} \propto |n-n_0|^{-6}$ and $\mu_n^{(y,z)} \propto |n-n_0|^{-3}$. The power-law decay is in accord with other models that possess long-range interaction [42–44]. As χ increases and the dipole-dipole interaction becomes more prominent. At this point we notice that the decay law becomes faster than the power law [see Fig. 4(b)]. This can be attributed to the fact that the array does not possess the discrete translational invariance. Although the absence of this symmetry is felt rather weakly, it becomes more and more pronounced as the coupling constant χ increases. Moreover, it should manifest itself in the strongest way at the edges of the array, since

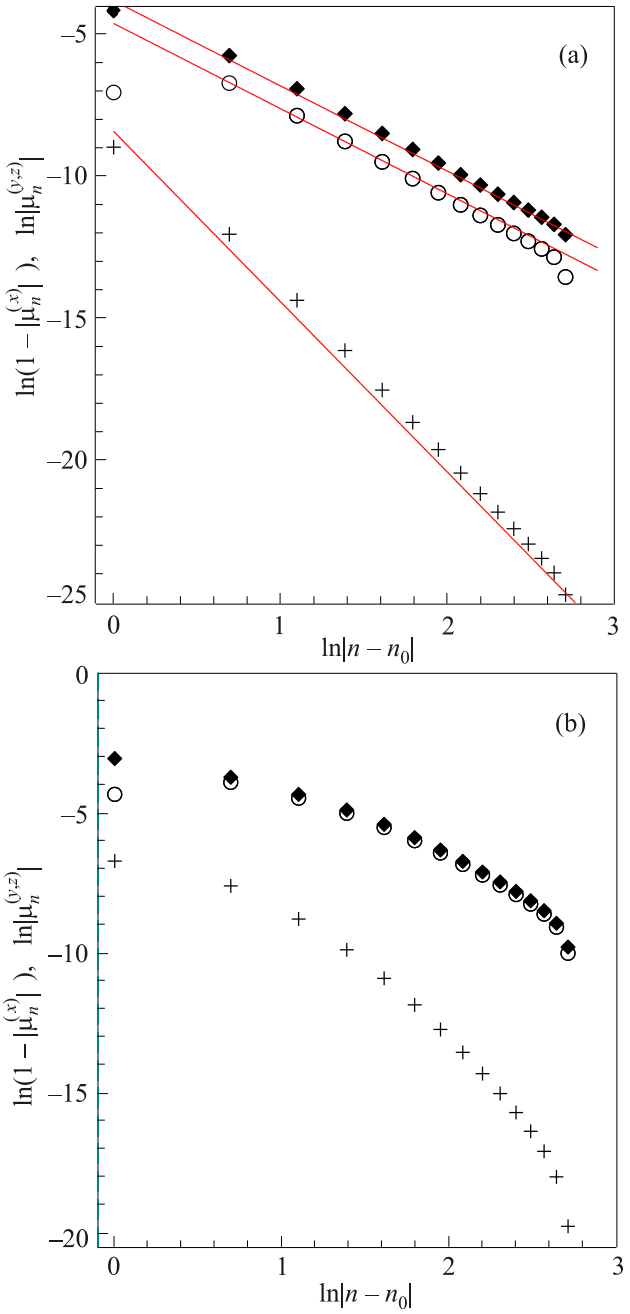

Fig. 4. (Color online) Spatial decay of the breather profile [$1 - |\mu_n|^{(x)}$ (+), $\mu_n^{(y)}$ (♦), $\mu_n^{(z)}$ (○)] on the log-log scale for the array of $N = 31$ dots with $\omega = 0.75$ and $\chi = 0.018$ (a) and $\chi = 0.048$ (b). The solid lines in the panel (a) approximate the decay of the magnetization (see text for details).

the dipoles at the edges interact only with the dipoles to the left (to the right), while the dipoles in the middle of the array interact symmetrically with all their neighbours. We remind, that the discrete translational invariance is possible only when the periodic boundary conditions are imposed.

Suppose we are not looking for the breather periodic orbit. Instead, we are simply interested in the details of the time evolution of the initial configuration (5) on the large time scale. Then we obtain the quasiperiodic localized solution. Its spatial structure will be the same as for the breathers, discussed in the previous paragraphs. The time evolution of the magnetization components appears to be quasiperiodic, as shown in Fig. 5. Here we have excited initially $N_r = 5$ dipoles with the precession frequency $\omega = 0.75$. As the course of evolution the localized structure persisted, but the temporal evolution exhibits two frequencies: the precession frequency $\omega \sim 0.75$ and the much lower envelope frequency. Within of one modulation period the magnetic moment can encompass the hard axis approximately ten times. It is not possible to trace the quasiperiodic breather solution with the method used in this section for the periodic breathers. The problem of the quasiperiodic breather existence is an interesting problem on its own [45,46] and will be pursued independently.

4. Discussion and conclusions

Discrete breathers (intrinsic localized modes) have been demonstrated to exist in the one-dimensional array of magnetic dots that interact as magnetic dipoles. We have focused on the arrays with the easy plane anisotropy. DBs are time periodic and spatially localized solutions of the Landau–Lifshitz equation. The structure of the breather solution is as follows: several dipoles in the core of the breather rotate around the hard axis and the rest perform small amplitude oscillations while lying in the easy plane. It should be noted that this type of breathers has no analogue in the continuum limit. The breather frequency should not resonate with the linear modes of the array (magnons). It appears that the area of breather existence is limited from below by the maximal frequency of the magnon band and by the value $\omega = 1$ (in the dimensionless units) from above.

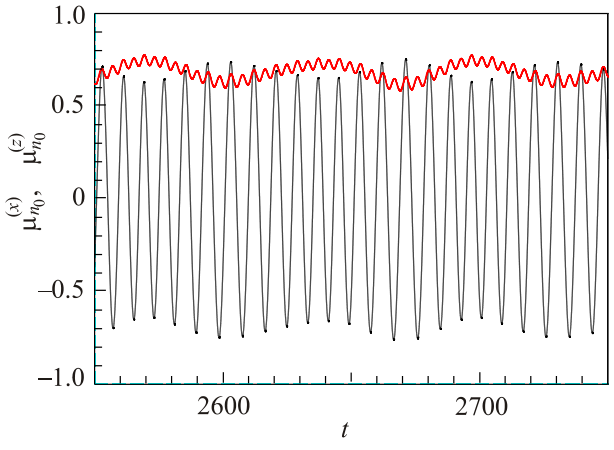

Fig. 5. (Color online) Temporal dynamics of the out-of-plane precessing magnetic moment components $\mu_n^{(x)}$ (black) and $\mu_n^{(z)}$ (red) in the array with $N = 31$ dots and $\chi = 0.25$, $N_r = 5$.

In terms of the structure and the existence conditions the solutions obtained in this article are similar to the DBs in classical ferromagnetic Heisenberg chains with the easy-plane anisotropy, obtained earlier [29,30]. The difference is that in the Heisenberg chains the ground state is degenerate while for the array of magnetic dipoles it is constrained to the state $\mu_n^{(x)} = 1$. Another difference appears due to the long-range dipole-dipole interaction, and it manifests itself in the asymptotic behaviour of the magnetization away from the breather core. Also, we believe that experimental observation of DBs in the arrays of magnetic particles seems to be much more easier as compared to the previously studied Heisenberg models. While in both models (Heisenberg and magnetic dots) the breathers exist if the interaction is considerably weaker than the anisotropy, such a situation is rather rare for the Heisenberg lattices, where the exchange interaction usually dominates over the anisotropy energy. In the case of magnetic dots the interaction can be chosen sufficiently weak by increasing the distance between the particles.

As far as the further research is concerned, we believe that the following directions are of considerable interest: (i) the influence of dissipation and external magnetic fields (both constant and periodic) on the breather existence area; (ii) DB existence and properties in arrays with easy-axis anisotropy; (iii) breather existence in the two-dimensional arrays of magnetic particles.

We thank V.P. Kravchuk for useful discussions. One of the authors (Y.Z.) acknowledges the financial support from the Ukrainian State Grant for Fundamental Research No. 0112U000056.

1. S.Y. Chou, M.S. Wei, P.R. Krauss, and P.B. Fischer, *J. Appl. Phys*. **76**, 6673 (1994).
2. G. Meier, M. Kleiber, D. Grundler, D. Heitmann, and R. Wiesendanger, *Appl. Phys. Lett*. **72**, 2168 (1998).
3. M. Grimsditch, Y. Jaccard, and I.K. Schuller, *Phys. Rev. B* **58**, 11539 (1998).
4. J.Y. Cheng, C.A. Ross, V.Z.-H. Chan, E.L. Thomas, R.G.H. Lammertink, and G.J. Vancso, *Adv. Mater*. **13**, 1174 (2001), ISSN 1521-4095 .
5. C.A. Ross, M. Hwang, M. Shima, J.Y. Cheng, M. Farhoud, T.A. Savas, H.I. Smith, W. Schwarzacher, F.M. Ross, M. Redjdal, F.B. Humphrey, *Phys. Rev. B* **65**, 144417 (2002).
6. C.A. Ross, S. Haratani, F.J. Castano, Y. Hao, M. Hwang, M. Shima, J.Y. Cheng, B. Vögeli, M. Farhoud, M. Walsh, *Henry I. Smith, J. Appl. Phys*. **91**, 6848 (2002).
7. P.V. Bondarenko, A.Y. Galkin, B.A. Ivanov, and C.E. Zaspel, *Phys. Rev. B* **81**, 224415 (2010).

8. R. Verba, G. Melkov, V. Tiberkevich, and A. Slavin, *Appl. Phys. Lett.* **100**, 192412 (2012).
9. T. Shinjo, T. Okuno, R. Hassdorf, K. Shigeto, and T. Ono, *Science* **289**, 930 (2000).
10. M. Natali, I.L. Prejbeanu, A. Lebib, L.D. Buda, K. Ounadjela, and Y. Chen, *Phys. Rev. Lett.* **88**, 157203 (2002).
11. S. Dzian and B. Ivanov, *Sov. Phys. JETP* **115**, 854 (2012).
12. A.M. Kosevich, B.A. Ivanov, and A.S. Kovalev, *Phys. Rep*. **194**, 117 (1990).
13. H.-J. Mikeska and M. Steiner, *Adv. Phys*. **40**, 191 (1991).
14. L.D. Faddeev and L.A. Takhtadjan, *Hamiltonian Methods in the Theory of Solitons*, Springer-Verlag, Berlin, Heidelberg, New York (2007).
15. A.A. Ovchinnikov, *Sov. Phys. JETP* **30**, 147 (1970).
16. A.M. Kosevich and A.S. Kovalev, *Sov. Phys. JETP* **67**, 1793 (1974).
17. R.S. MacKay and S. Aubry, *Nonlinearity* **7**, 1623 (1994).
18. S. Aubry, *Physica D* **103**, 201 (1997).
19. S. Flach and C.R. Willis, *Phys. Rep*. **295**, 182 (1998).
20. R. Lai and A.J. Sievers, *Phys. Reps*. **314**, 147 (1999).
21. S. Flach and A.V. Gorbach, *Phys. Reps*. **467**, 1 (2008), ISSN 0370-1573.
22. H. Segur and M.D. Kruskal, *Phys. Rev. Lett*. **58**, 747 (1987).
23. S. Flach, *Phys. Rev. E* **50**, 3134 (1994).
24. S. Flach, *Phys. Rev. E* **51**, 1503 (1995).
25. B.A. Ivanov, A.M. Kosevich, and I.M. Babich, *JETP Lett*. **29**, 714 (1979).
26. S. Rakhmanova and A.V. Shchegrov, *Phys. Rev. B* **57**, R14012 (1998).
27. S. Rakhmanova and D.L. Mills, *Phys. Rev. B* **58**, 11458 (1998).
28. S. Takeno and K. Kawasaki, *J. Phys. Soc. Jpn*. **60**, 1881 (1991).
29. Y. Zolotaryuk, S. Flach, and V. Fleurov, *Phys. Rev. B* **63**, 214422 (2001).
30. J.M. Khalack, Y. Zolotaryuk, and P.L. Christiansen, *Chaos* **13**, 683 (2003).
31. M. Lakshmanan, M. Subash, and A. Saxena, *Phys. Lett. A* **378**, 1119 (2014).
32. B. Tang, D.-J. Li, and Y. Tang, *Phys. Scripta* **89**, 095208 (2014).
33. B. Tang, D.-J. Li, and Y. Tang, *Chaos* **24**, 023113 (2014).
34. R. Lai and A.J. Sievers, *Phys. Rev. Lett*. **81**, 1937 (1998).
35. U.T. Schwarz, L.Q. English, and A.J. Sievers, *Phys. Rev. Lett*. **83**, 223 (1999).
36. M.V. Gvozdikova and A.S. Kovalev, *Fiz. Nizk. Temp*. **24**, 1077 (1998) [*Low Temp. Phys*. **24**, 808 (1998)].
37. M.V. Gvozdikova, *Fiz. Nizk. Temp*. **25**, 1295 (1999) [*Low Temp. Phys*. **25**, 972 (1999)].
38. A.I. Akhiezer, V.G. Baryakhtar, and S.V. Peletminskii, *Spin Waves*, North-Holland Publishing Company, Amsterdam (1968).
39. J.F. Epperson, *An Introduction to Numerical Methods and Analysis*, John Wiley and Sons, Inc., Hoboken, New Jersey (2007).
40. S. Flach and A. Gorbach, *Internat. J. Bifurcat. Chaos* **16**, 1645 (2006).
41. A.E. Miroshnichenko, S. Flach, M.V. Fistul, Y. Zolotaryuk, and J.B. Page, *Phys. Rev. E* **64**, 066601 (2001).
42. Y.B. Gaididei, S.F. Mingaleev, P.L. Christiansen, and K.O. Rasmussen, *Phys. Rev. E* **55**, 6141 (1997).
43. M. Johannson, Y.B. Gaididei, P.L. Christiansen, and K.O. Rasmussen, *Phys. Rev. E* **57**, 4739 (1998).
44. K.O. Rassmussen, P.L. Christiansen, M. Johansson, Y.B. Gaididei, and S.F. Mingaleev, *Physica D* **113**, 134 (1998).
45. D. Bambusi and D. Vella, *Dyn. Sys. Ser. B* **2**, 389 (2002).
46. J. Geng, J. Viveros, and Y. Yi, *Physica D* **237**, 2866 (2008).